Available online at www.sciencedirect.com

SCIENCE DIRECT®

Journal of Photochemistry and Photobiology A: Chemistry 171 (2005) 181–186

Journal of Photochemistry and Photobiology A:Chemistry

www.elsevier.com/locate/jphotochem

Photophysical properties of dysprosium complexes with aromatic carboxylic acids by molecular spectroscopy

Bing Yan*, Bing Zhou

Department of Chemistry, Tongji University, Shanghai 200092, P.R. China

Received 17 July 2004; received in revised form 1 October 2004; accepted 13 October 2004
Available online 21 November 2004

Abstract

A series of luminescent dysprosium complexes with different aromatic carboxylic acids have been synthesized and characterized. The photophysical properties of these complexes have been studied with all kinds of molecular spectroscopy such as infrared spectra, ultraviolet spectra, phosphorescence spectra and fluorescence spectra. Especially the energy match and intramolecular energy transfer process between the triplet state energies of aromatic carboxylic acids and the resonant emissive energy level of Dy^{3+} was discussed in detail for the first time. Which indicates that the heterocyclic aromatic carboxylic acids (pyridine-carboxylic acids) are more suitable for the luminescence of Dy^{3+} than benzoic acid derivatives.

Keywords: Dysprosium complexes; Aromatic carboxylic acids; Photophysical properties; Molecular spectroscopy; Energy match; Intramolecular energy transfer

1. Introduction

The photophysical properties of rare earth coordination compounds with organic ligands have been the subject of great interest because these functional complexes have great potential applications in such fields as the active center of luminescent materials [1–3] or as structural and functional probe for the chemical and biological macromolecule systems [4–6]. A lot of reports were focused on the luminescence, energy match and intramolecular energy transfer mechanism of rare earth complexes with β-diketones, aromatic carboxylic acids and heterocyclic ligands, which show good energy coupling and, afterwards good luminescent properties of rare earth ions [7–10]. We also have studied the energy match and intramolecular energy transfer mechanism of binary and ternary lanthanide complexes with aromatic carboxylic acids and 1,10-phenanthroline in detail [11–14]. The luminescence properties of rare earth complexes depend mainly on the intramolecular energy transfer efficiency from organic ligand to the central rare earth ions. Among the factors affecting the efficiency, the energy match between the triplet state energies of organic ligands and the resonant energy levels of rare earth trivalent ions is the most important. Especially rare earth complexes of aromatic carboxylic acids have higher thermal or luminescent stabilities for practical applications than other lanthanide systems because they readily form the dimer or infinite chain polymeric structures [15–20]. But the most research was mainly reported on the europium and terbium complexes systems, and little attention has been paid on dysprosium complexes of aromatic carboxylic acids [7–14,21]. Dysprosium ion exhibits characteristic blue and yellow emissions locating at around 484 and 575 nm, separately, which are corresponded to the characteristic $^4F_{9/2} \rightarrow {}^6H_J$ ($J = 15/2$, 13/2) transitions of Dy^{3+}. The suitable control of blue/yellow intensity ratio can be expected to realize a white luminescent system. In the context, a series of 12 dysprosium complexes were synthesized and the corresponding photophysical properties were studied in detail.

---

* Corresponding author. Tel.: +86 2165984663; fax: +86 2165982287.
E-mail address: byan@tongji.edu.cn (B. Yan).

1010-6030/$ – see front matter © 2004 Elsevier B.V. All rights reserved.
doi:10.1016/j.jphotochem.2004.10.012

Table 1
Elemental analysis data for Dy complexes

Dysprosium complexes	Found (%)			Calculated (%)		
	C	H	N	C	H	N
$Dy(OABA)_3(H_2O)_2$	41.21	3.26	7.14	41.55	3.63	6.92
$Dy(PABA)_3(H_2O)_2$	41.27	3.31	6.79	41.55	3.63	6.92
$Dy(AMBA)_3(H_2O)_3$	43.09	4.36	6.47	43.22	4.53	6.30
$Dy(OMBA)_3(H_2O)_2$	48.14	3.88		47.72	4.14	
$Dy(MMBA)_3(H_2O)_3$	48.03	3.86		47.72	4.14	
$Dy(NIC)_3(H_2O)_2$	38.61	2.55	7.69	38.28	2.86	7.44
$Dy(PIC)_3(H_2O)_2$	38.69	2.61	7.75	38.28	2.86	7.44
$Dy(BA)_3(H_2O)_4$	48.02	3.62		48.21	3.88	
$Dy(OCBA)_3(H_2O)$	39.25	2.04		38.96	2.16	
$Dy(SAL)_3(H_2O)_4$	41.13	2.98		41.35	3.12	
$Dy(TBUBA)_3$	56.87	5.42		57.10	5.66	

2. Experimental

Dy_2O_3 was converted to its nitrate by treating with concentrated nitric acid. The dysprosium complexes with aromatic carboxylic acids were prepared by homogeneous precipitation. The pH value of the mixed ethanol/water solutions of aromatic carboxylic acids was adjusted to be about 6.5 using sodium hydroxide. After stirring, dysprosium nitrate were dipped and then white precipitates appeared. The resulting solid was filtered off, washed with ethanol and water, dried and stored over silica gel.

Elemental analysis (C, H, N) was carried out by an Elementar Cario EL elemental analyzer. Infrared spectroscopy on KBr pellets was performed on a Nicolet Nexus 912 AO446 model spectrophotometer in the range of 4000–400 cm^{-1}. Ultraviolet absorption spectra of these complexes ($5 \times 10^{-4}\,\mathrm{mol\,L}^{-1}$ ethanol solution) were recorded with an Agilent 8453 spectrophotometer. Luminescence (excitation and emission) spectra of these solid complexes and phosphorescence spectra ($5 \times 10^{-4}\,\mathrm{mol\,L}^{-1}$ ethanol solution) at nitrogen atmosphere were determined with a Perkin-Elmer LS-55 spectrophotometer whose excitation and emission slits were 10 and 5 nm, respectively.

3. Results and discussion

The compositions of the complexes were confirmed by elemental analyses (shown in Table 1) and led to $Dy(A)_3(H_2O)_x$, where A = pyridine-3-carboxylate (NIC), pyridine-4-carboxylate (PIC), 2,6-pyridine-dicarboxylate (HDPA), *ortho*, *para* aminobenzoate (O(M,P)ABA), *ortho*, *meta*, methyl aminobenzoate acid (O(M)MBA), ortho cholobenzoic acid (OCBA), 3-amino-4-methylbenzoate (AMBA), 4-*tert*-butylbenzoate (TBBA), benzoate (BA) and *ortho*-hydroxylbenozate (SAL); $x = 2$–4.

All the IR spectra of these dysprosium complexes show the similar features. Compared the IR spectra of free aromatic carboxylic acids and their dysprosium complexes, the characteristic absorption bands of C=O and C–O bands belonging to the free carboxylic acids ligands disappear, while the characteristic absorption peaks of carboxylic group COO^- appear, which suggest that the oxygen atoms of carbonyl groups of aromatic carboxylic acids are coordinated with Dy^{3+}. Besides, it can be observed that the absorption frequencies of Ln–O bond lie at around 400 cm^{-1} in the low frequency of IR spectra for some dysprosium complexes systems. It is worthy pointing out that there exist some differences in IR spectra for H_2O molecules in different dysprosium com-

Table 2
The IR absorption bands of dysprosium complexes with aromatic carboxylic acids

Dysprosium complexes	$V_{\mathrm{S,COO}^-}$ (cm^{-1})	$V_{\mathrm{aS,COO}^-}$ (cm^{-1})	V_{H_2O} (cm^{-1})		
$Dy(OABA)_3(H_2O)_2$	1395	1513	3397	1623	595
$Dy(PABA)_3(H_2O)_2$	1417	1522	3405	1602	595
$Dy(AMBA)_3(H_2O)_3$	1525	1524	3385	1623	595
$Dy(OMBA)_3(H_2O)_2$	1404	1522	3433	1623	595
$Dy(MMBA)_3(H_2O)_3$	1396	1522	3433	1609	588
$Dy(NIC)_3(H_2O)_2$	1424	1548	3377	1602	581
$Dy(PIC)_3(H_2O)_2$	1413	1548	3398	1602	588
$Dy(HDPA)_3(H_2O)_2$	1424	1553	3433	1595	587
$Dy(BA)_3(H_2O)_4$	1416	1520	3426	1602	588
$Dy(OCBA)_3(H_2O)$	1411	1527	3426	1602	602
$Dy(SAL)_3(H_2O)_4$	1396	1535	3398	1623	588
$Dy(TBUBA)_3$	1414	1520	3433	1602	

plexes. For example, some apparent bands are noted at about 3450 and 1613 cm^{-1} in IR spectra of $Dy(TBBA)_3(H_2O)_2$, which are respectively attributed to the stretching vibration band and in-plane bending band of H_2O molecules. The absorption bands corresponded to the in-plane swing vibration of coordinated H_2O molecules have not been observed in the range of 605–585 cm^{-1}, which verifies that the water molecule is not coordinated to Dy^{3+} and corresponds to crystal water molecule [15]. While other dysprosium complexes show some in-plane swing vibration of coordinated H_2O molecules, the similar features have been observed in the range of 605–575 cm^{-1}, which verifies there exist both coordinated water molecules and crystal water molecules in these dysprosium complexes [15]. Table 2 gives the detailed data for the main absorption bands and assignments.

Fig. 1 shows the ultraviolet absorption spectra for dysprosium complexes with benzoates derivatives: dysprosium complexes of aminobenzoates (A), dysprosium complexes of methylbenzoates (B), and dysprosium complexes of other benzoate derivatives (C), respectively. For Fig. 1(A), both $Dy(OABA)_3(H_2O)_2$ and $Dy(PABA)_3(H_2O)_2$ show the similar absorption band except for a little distinction of intensities, corresponding to the same substituted amino group with different substituted position. While $Dy(AMBA)_3(H_2O)_3$ shows some band shift for the existence of substituted methyl group besides amino group. For Fig. 1(B), both $Dy(OMBA)_3(H_2O)_2$ and $Dy(MMBA)_3(H_2O)_3$ show the similar absorption band except for a little difference of intensities for the same substituted methyl group with different substituted position. While $Dy(AMBA)_3(H_2O)_3$ show some shift because of the three-substituted amino group besides methyl groups. For Fig. 1(C), dysprosium complexes of benzoate derivatives with different substituted groups show different ultraviolet absorption bands. Different aromatic carboxylic acids molecules with different substituted groups have great influence on the electron distribution and the properties of electron donor and acceptor of the corresponding delocalized conjugated systems, which gives rise to the change of ultraviolet absorption and the band shift of ultraviolet spectra. Coordinated to Dy^{3+}, the more extensive conjugated systems form between ligands and central Dy^{3+}, leading to the more delocalized electron distribution and the red-shift of ultraviolet spectra. Fig. 2 shows the ultraviolet absorption spectra dysprosium complexes of pyridine-carboxylates, which shows the similar feature to the above benzoate derivatives. The heterocylic nitrogen atom causes the absorption band shift compared to phenyl cycle. The absorption bands at 257 (257, 255) and 273 nm can be attributed to the characteristic absorption of pyridine group.

Molecular phosphorescence reflects to the excited state characteristic of organic molecules and different phosphorescent emission bands correspond to the different aromatic carboxylic acids ligands. So the excited triplet state energies of aromatic carboxylic acids can be determined with their phosphorescence spectra. The low temperature phosphorescence spectra of these aromatic carboxylic acids were measured at nitrogen atmosphere (77 K) (as shown in Figs. 3 and 4) and the triplet state energy of them can be determined based on the maximum phosphorescence band. The energy differences between the triplet state of aromatic carboxylic acids and the resonant energy level of Dy^{3+} ($^4F_{9/2}$, 21,000 cm^{-1}) can be calculated and the detailed data have been shown in Table 3. From these energy differences, it can be seen that all these ligands can sensitize dysprosium ion effectively. According to the intramolecular energy mechanism [20–22], the intramolecular energy transfer efficiency depends chiefly on two energy transfer processes: the first one leads from the triplet level of ligands to the emissive energy level of the Ln^{3+}

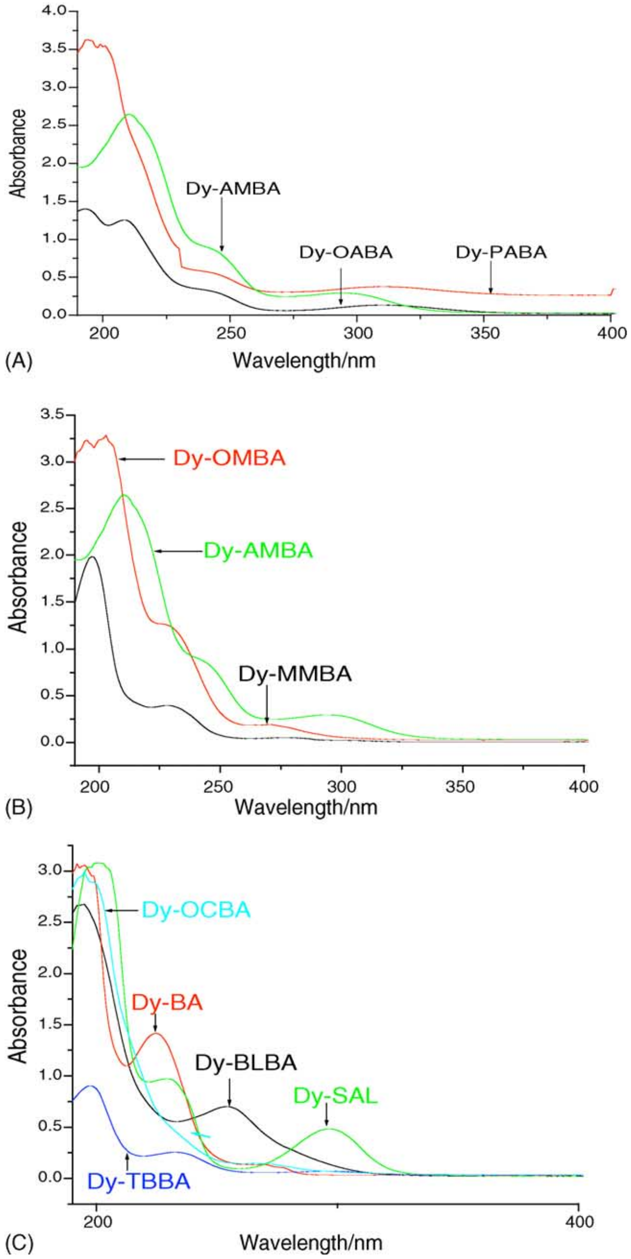

Fig. 1. Ultraviolet absorption spectra of dysprosium complexes of benzoic acids derivatives. (A) Dy-aminobenzoate derivatives, (B) Dy-methylbenzoate derivatives, (C) Dy-other benzoate derivatives.

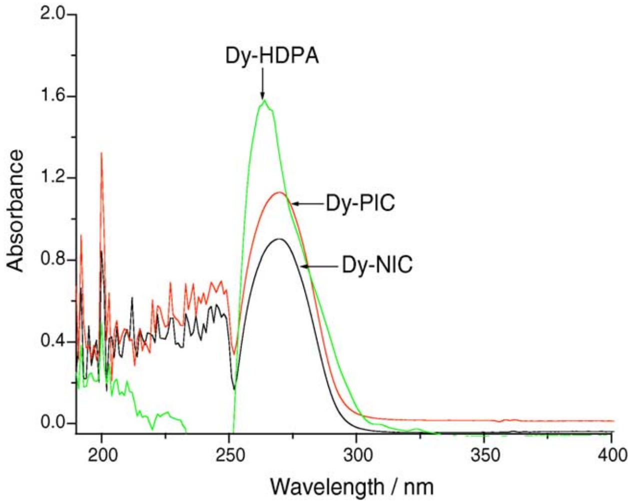

Fig. 2. Ultraviolet absorption spectra of dysprosium complexes of pyridinecarboxylic acids.

ion by Dexter's resonant exchange interaction; the second one is just an inverse energy transfer by a thermal deactivation mechanism. Both energy transfer rate constants depend on the energy differences between the triplet level of the ligands and the resonant emissive energy of Ln^{3+}. Intramolecular energy transfer efficiency in lanthanide complexes conforms to Dexter's exchange energy transfer theory [23]:

$$K_{\mathrm{ET}} = \left(\frac{2\pi Z^2}{R}\right) \exp(-2r/l) \int F_{\mathrm{d}}(E) F_{\mathrm{a}}(E)\,\mathrm{d}E \qquad (1)$$

K_{ET} is the rate constant of energy transfer, r the intermolecular distance between the energy donor and acceptor atoms, l the *van der Waals* radius, the integral represents the overlap between the luminescence spectrum of the ligands and the absorption spectrum of Ln^{3+}, $F_{\mathrm{d}}(E)$ the luminescence spectrum of energy donor (ligand), $F_{\mathrm{a}}(E)$ the absorption spectrum of energy acceptor (Dy^{3+}), and $2\pi Z^2/R$ is a constant relating to the mutual distance between Dy^{3+} and coordinated atom. r and l are both considered to be constant for intramolecular energy transfer processes. From Eq. (1), with the decrease of energy difference ΔE(Tr-Dy^{3+}) between the triplet state energy of ligands and the resonance emission energy of Dy^{3+}, the overlap between the luminescence spectrum of energy donor (ligand) $F_{\mathrm{d}}(E)$ and the absorption spectrum of energy acceptor (Dy^{3+}) $F_{\mathrm{a}}(E)$ increases. Subsequently, K_{ET} increases for it is directly proportional to the overlap integral of $F_{\mathrm{d}}(E)$ and $F_{\mathrm{a}}(E)$. Thus, ligands with a large energy difference cannot sensitize rare earth ions effectively for the overlap integral is too small to produce effective K_{ET}.

Table 3
The phosphorescence spectra data of aromatic carboxylic acids

Ligands	Triplet state energies (cm^{-1})	ΔE(Tr-Dy^{3+}) (cm^{-1})
HOABA	24752	3752
HPABA	24242	3242
HAMBA	23447	2447
HOMBA	25000	4000
HMMBA	23923	2923
HNIC	23256	2256
HPIC	24038	3038
HBA	23557	2557
HOCBA	23895	2895
HSAL	24184	3184
HTBUBA	24125	3125

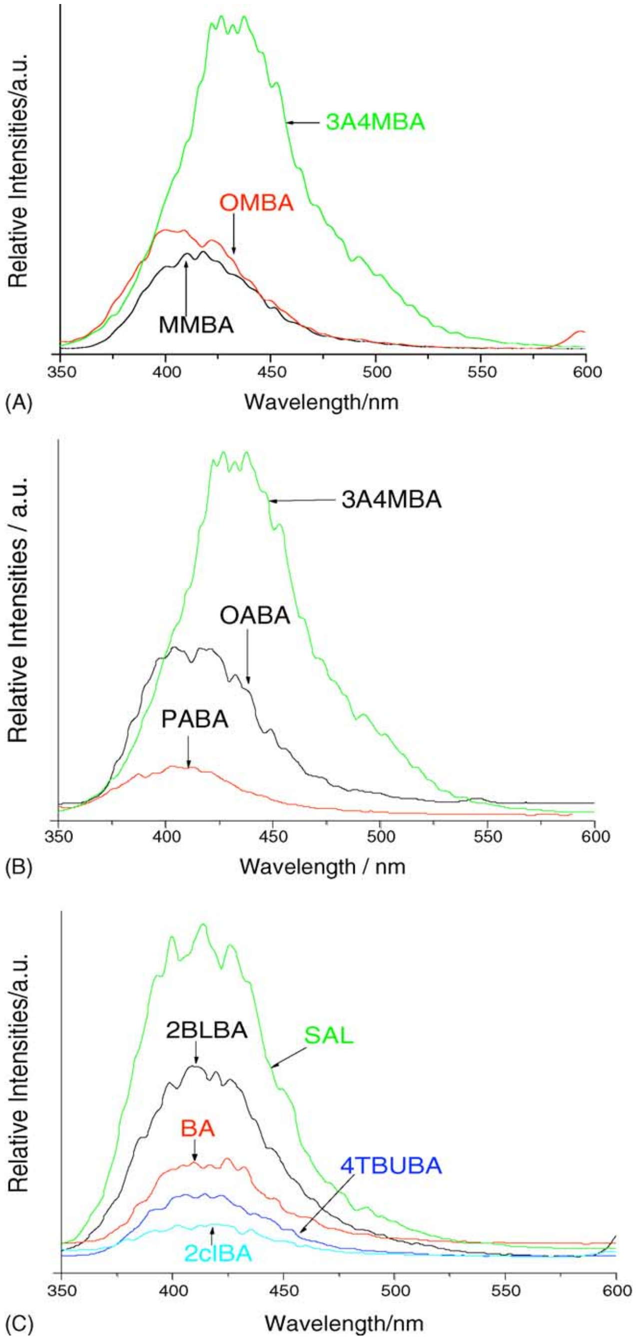

Fig. 3. Phosphorescence spectra of benzoic acids derivatives (A) aminobenzoic acids derivatives, (B) methylbenzoic acids derivatives, (C) other benzoic acids derivatives.

On the other hand, there exists an inverse energy transfer process which affects luminescence intensity by temperature

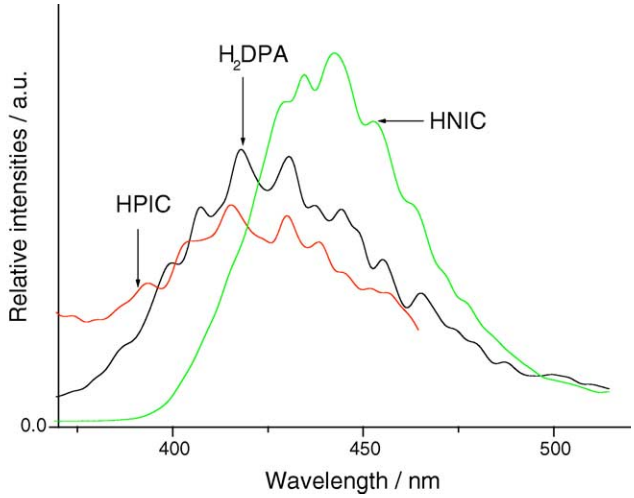

Fig. 4. Phosphorescence spectra of pyridine-carboxylic acids.

[24], $k(T)$ the rate constant of inverse energy transfer process (thermal deactivation process), A the pre-exponential factor:

$$K(T) = A \exp\left(-\frac{\Delta E(\text{Tr-Dy}^{3+})}{RT}\right) \qquad (2)$$

It can be seen that the activation energy is approximately equal to $\Delta E(\text{Tr-Dy}^{3+})$ in the inverse energy transfer process; therefore, a decreasing energy difference increases $k(T)$. Based on this evidence, the conclusion can be drawn that $\Delta E(\text{Tr-Dy}^{3+})$ is of opposite influence on the two energy transfer processes and an optimal value can be assumed to exist (around $3000 \pm 500\,\text{cm}^{-1}$). From the data in Table 3, it can be primarily predicted that the energy transfer between OABA, OMBA and Dy^{3+} is worse. Certainly the energy transfer is only one factor determining the luminescence properties of rare earth complexes, which also depend on the structure of ligands.

The excitation spectra of these complex systems show that there is no effective absorption in the 300–400 nm ultraviolet region. Fig. 5 gives the excitation spectrum of $Dy(HDPA)_3 \cdot H_2O$. The effective energy absorption mainly takes place in the narrow ultraviolet region of 200–280 nm. Four main excitation bands are located at 222, 242, 257 and 271 nm, respectively. We further measured the corresponding emission spectra by selective excitation into the four different components; they show a similar emission position except for different luminescent intensities. The emission spectra were measured in detail. Figs. 6 and 7 present the selected emission spectra of $Dy(PABA)_3(H_2O)_2$ (Fig. 6(A)), $Dy(AMBA)_3(H_2O)_2$ (Fig. 6(B)) and $Dy(HDPA)_3(H_2O)_2$ (Fig. 7), respectively. For $Dy(PABA)_3(H_2O)_2$ complex, the luminescence spectrum shows two apparent emission peaks under excitation at 242 nm: one is located at 481 nm and the other at 572.5 nm, corresponding to the characteristic ${}^4F_{9/2} \rightarrow {}^6H_J$ ($J = 15/2, 13/2$) emission transitions of Dy^{3+} ion. The detailed data about the relative intensities for the blue and yellow emission of Dy^{3+} in their complexes were summarized

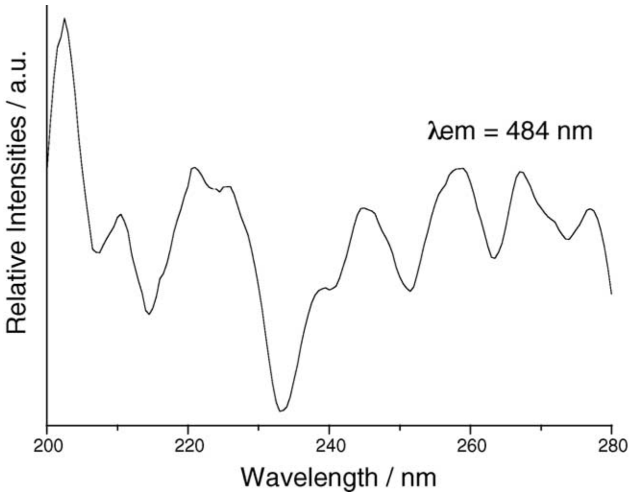

Fig. 5. Excitation spectrum of $Dy(HDPA)_3(H_2O)_2$.

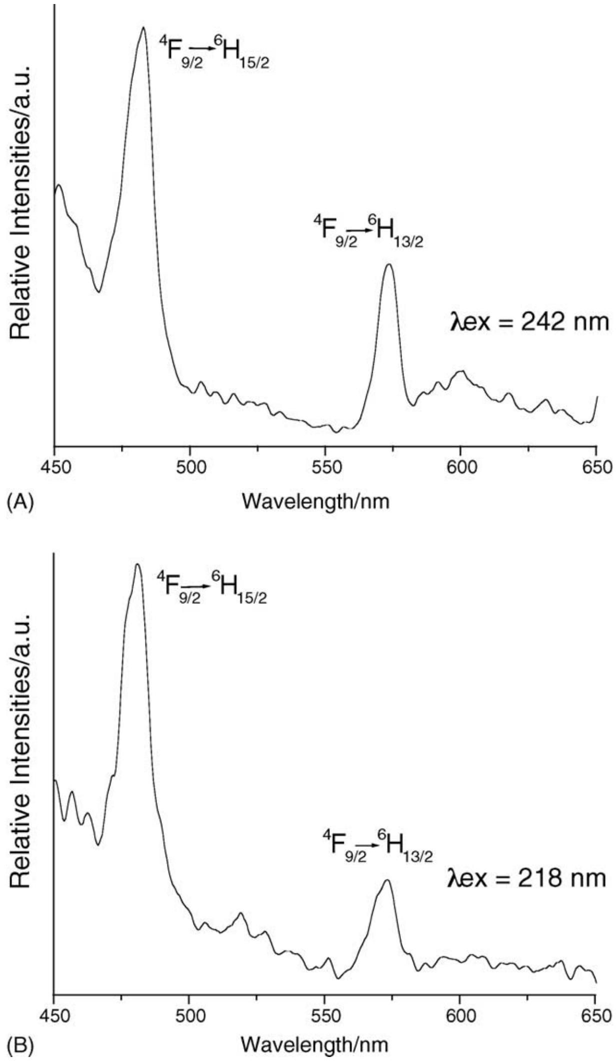

Fig. 6. Emission spectra of (A) $Dy(PABA)_3(H_2O)_2$ and (B) $Dy(AMBA)_3(H_2O)_2$.

Table 4
The luminescence intensities of dysprosium complexes of aromatic carboxylic acids

Complexes	Blue emission intensities (a.u.)	Yellow emission intensities (a.u.)
$Dy(OABA)_3(H_2O)_2$	48.1 (482 nm)	14.0 (573 nm)
$Dy(PABA)_3(H_2O)_2$	76.0 (483 nm)	33.0 (574 nm)
$Dy(AMBA)_3(H_2O)_3$	147 (481 nm)	39.2 (573.5 nm)
$Dy(OMBA)_3(H_2O)_2$	20.1 (483 nm)	3.93 (574.5 nm)
$Dy(MMBA)_3(H_2O)_3$	65.1 (482 nm)	21.5 (575.5 nm)
$Dy(NIC)_3(H_2O)_2$	522 (483 nm)	139 (574 nm)
$Dy(PIC)_3(H_2O)_2$	745 (483.5)	183 (574 nm)
$Dy(HDPA)_3(H_2O)_2$	983 (481 nm)	314 (572.5 nm)
$Dy(BA)_3(H_2O)_4$	154.7 (478.5 nm)	44.5 (571.5 nm)
$Dy(OCBA)_3(H_2O)$	79.2 (484.5 nm)	27.5 (573.5 nm)
$Dy(SAL)_3(H_2O)_4$	79.5 (482 nm)	26.9 (573 nm)
$Dy(TBUBA)_3$	69.5 (482.5 nm)	20.4 (573.5 nm)

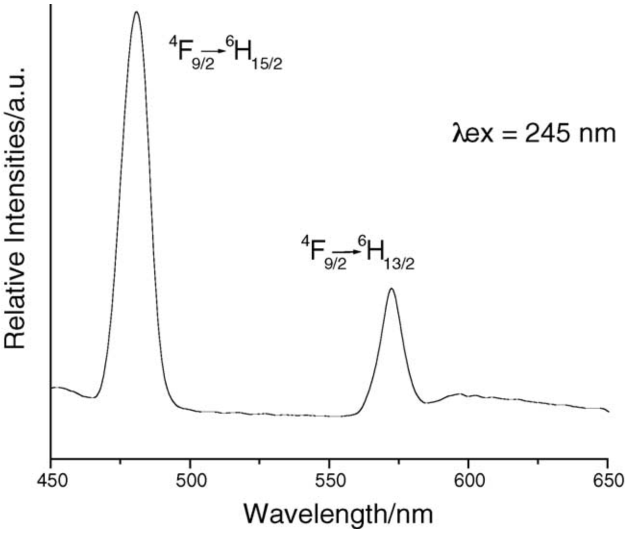

Fig. 7. Emission spectrum of $Dy(HDPA)_3(H_2O)_2$.

in Table 4. Both blue and yellow emission intensities of Dy^{3+} complexes with pyridine-carboxylic acids are stronger than those of Dy^{3+} complexes of benzoic acids derivatives, which suggests that the triplet state energies of pyridine-carboxylic acids are more suitable for the luminescence of Dy^{3+} than those of benzoic acids derivatives.

4. Conclusions

In summary, a series of dysprosium complexes with aromatic carboxylic acids have been synthesized and characterized. The photophysical properties of these systems have been studied with ultraviolet absorption, phosphorescent, fluorescent excitation and emission spectra. The energy match and intramolecular energy transfer between aromatic carboxylic acids and dysprosium ions were discussed in detail, which indicate that the pyridine-carboxylic acids are more suitable for the luminescence of Dy^{3+} than benzoic acids derivatives.

Acknowledgement

This work was supported by the Science Fund of Tongji University for Talented Researchers and the National Natural Science Foundation of China (20301013).

References

[1] P.A. Tanner, B. Yan, H.J. Zhang, J. Mater. Sci. 35 (2000) 4325.
[2] B. Yan, J.Y. You, J. Rare Earth 24 (2002) 404.
[3] B. Yan, Mater. Lett. 57 (2003) 2535.
[4] C.F. Meares, T.G. Wensel, Acc. Chem. Res. 17 (1984) 202.
[5] Y.X. Ci, Y.Z. Li, W.B. Chang, Anal. Chim. Acta 248 (1991) 589.
[6] L.K. Scott, W.D. Horrocks, J. Inorg. Biochem. 46 (1992) 193.
[7] Y.S. Yang, M.L. Gong, Y.Y. Li, H.Y. Lei, S.L. Wu, J. Alloys Compds. 207/208 (1994) 112.
[8] C.J. Feng, Q.H. Luo, C.Y. Duan, J. Chem. Soc., Dalton Trans. (1998) 377.
[9] T. Gunnlaugsson, A.J. Harte, J.P. Leonard, M. Nieuwenhuyzen, Chem. Commun. (2002) 2135.
[10] B. Yan, Y.S. Song, J. Fluoresc. 14 (2004) 289.
[11] H.J. Zhang, B. Yan, S.B. Wang, J.Z. Ni, J. Photochem. Photobiol. A: Chem. 109 (1997) 223.
[12] B. Yan, H.J. Zhang, S.B. Wang, J.Z. Ni, Spectrosc. Lett. 31 (1998) 603.
[13] B. Yan, H.J. Zhang, S.B. Wang, J.Z. Ni, Monatsh. Chem. 129 (1998) 151.
[14] B. Yan, H.J. Zhang, S.B. Wang, J.Z. Ni, Monatsh. Chem. 129 (1998) 567.
[15] B. Yan, H.J. Zhang, S.B. Wang, J.Z. Ni, J. Photochem. Photobiol. A: Chem. 116 (1998) 209.
[16] B. Yan, Q.Y. Xie, Inorg. Chem. Commun. 6 (2003) 1448.
[17] B. Yan, Q.Y. Xie, J. Coord. Chem. 56 (2003) 1289.
[18] B. Yan, Q.Y. Xie, J. Mol. Struct. 688 (2004) 73.
[19] B. Yan, Y.S. Song, Z.X. Chen, J. Mol. Struct. 694 (2004) 115.
[20] S. Sato, M. Wada, Bull. Chem. Soc. Jpn. 43 (1970) 1955.
[21] B. Yan, H. Shao, H.J. Zhang, S.B. Wang, J.Z. Ni, Chin. J. Inorg. Chem. 14 (1998) 407.
[22] B. Yan, H.J. Zhang, J.Z. Ni, Chem. Res. Chin. Univ. 14 (1998) 245.
[23] D.L. Dexter, J. Chem. Phys. 21 (1953) 836.
[24] C.R.S. Dean, T.M. Shepherd, J. Chem. Soc., Faraday Trans. II 71 (1975) 146.